

# Comprehensive Framework for Dynamic Quadruped Locomotion

Ibraheem Al-Tameemi, Ethan Chandler, Hushmand Esmaeili, Varun Walimbe

**Abstract**—This paper presents a control framework for a quadruped robot to perform smooth dynamic locomotion. The forward kinematics (FK) and inverse kinematics (IK) solution is derived for the proposed robot to formulate the relationship between the foot-tip of the leg and the base of the robot. By deriving a continuous kinematic phase function for various gait templates, the approach puts the framework in the unique position of achieving superior gait transitions in terms of smoothness and stability. Additionally, by loosening the number of constraints on footstep positions, the planner is able to identify optimal swing-phase trajectories via Bézier curves, enabling the body to follow a reference velocity via a state-of-the-art MPC/WBIC pipeline.

## I. INTRODUCTION

In recent years, legged robotics has been an active research field. Due to their distinctive motion shape, control mechanism, and adaptation to complicated situations, bio-inspired foot robots have become a topic of interest within the field of robot research. The stability and load capacity of quadruped robots are significantly superior to those of biped robots. The mechanism and control strategy complexity is less than that of hexapod and multi-legged robots. Thus, quadruped robots have numerous applications in military transportation, forest identification, and emergency rescue.

Achieving dynamic locomotion with legged robots in such real-life environments is challenging. The problem can be extended to locomotion in rough terrain, which introduce greater external disturbances, and even recovery from pushing or slippage. Different speeds or terrains may then require different gaits and even compliant legs.

Current solutions for highly dynamic locomotion have yielded impressive results. The Mini Cheetah quadruped developed by MIT proposed a novel control framework [1], which combines a newly devised whole-body impulse control (WBIC) and model predictive control (MPC). Although previous WBIC formulations focus on tracking center of mass (CoM) trajectories, WBIC incorporates both body posture stabilization and reaction forces formulation. The MPC then finds the reaction forces required by the WBIC. The control framework was tested on six different gaits in different environments. [5] propose an implementation of MPC to determine ground reactions for a quadruped robot. The main contribution is a controller that can stabilize a large number of gaits. Experimental results demonstrated control of gaits including stand, trot, pronk, bound, and others.

Despite major advancements in control frameworks for achieving dynamic locomotion, there is still a lack of research on the generation of a continuous time gait. Thus, defining a constant duty factor might cause a jerky gait transition. This paper proposes a control framework that

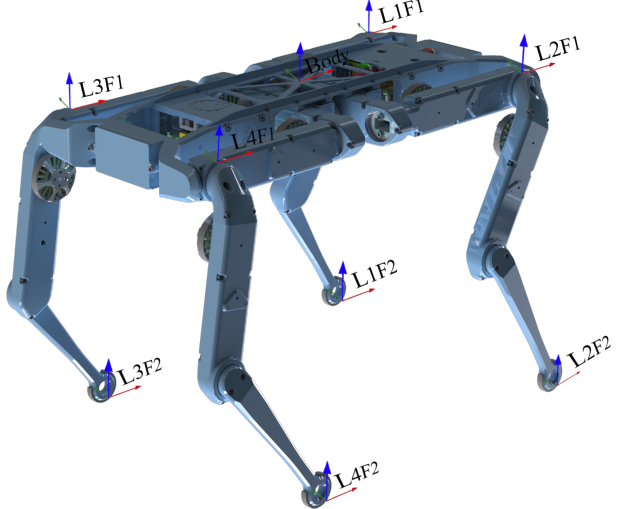


Fig. 1. Solo-12 Frames

relies on a continuous time function for the gait generation to achieve a smooth dynamic locomotion of the quadruped robot.

This paper is organized as follows. Section II describes the basic system architecture and conventions used in this paper for the Solo-12. The kinematics are presented in Section III, followed by the control problem formulation in Section IV, while Section V contains implementation details. Section VI contains experimental results, with research conclusions and future work discussed in Section VII.

## II. ARCHITECTURE

### A. Solo-12

The Solo-12 quadruped is an open-hardware 12-DOF robot developed by Open Dynamic Robot Initiative [3]. The robot features 12 Antigravity 4004 300kV BLDC motors, which are driven by 6 MicroDriver v2's, with a Launchpad F28069M to provide FOC. The robot is high-performance and low-cost, making it desirable for research purposes.

### B. Conventions

The body and local leg coordinate systems are defined in Figure 1, where the red, green, and blue basis vectors correspond to the x-axis, y-axis, and z-axis of each frame respectively. Additionally, all vectors in this paper are bold, upright, and lowercase ( $\mathbf{a}$ ,  $\boldsymbol{\omega}$ ), matrices are bold, upright, and uppercase ( $\mathbf{A}$ ,  $\boldsymbol{\Omega}$ ), and scalars are lowercase and italicized ( $a$ ,  $\omega$ ). Finally,  $\mathbf{1}_n$  is used to denote an  $n \times n$  identity matrix.

### III. KINEMATICS

In swing phase, each leg can be modeled as an independent 3-DOF serial linkage. In this section, we will briefly cover the kinematic solution of this model for the sake of completeness.

#### A. Leg Forward Kinematics

The forward kinematics of each leg are given by the following equations:

$$\mathbf{x}_{\text{foot tip}}^{\text{hip}} = -\cos(\theta_1)(L_4 \cos(\theta_2 + \theta_3) - L_2 + L_3 \cos(\theta_2)) \quad (1)$$

$$\mathbf{y}_{\text{foot tip}}^{\text{hip}} = -\sin(\theta_1)(L_4 \cos(\theta_2 + \theta_3) - L_2 + L_3 \cos(\theta_2)) \quad (2)$$

$$\mathbf{z}_{\text{foot tip}}^{\text{hip}} = L_1 - L_4 \sin(\theta_2 + \theta_3) - L_3 \sin(\theta_2) \quad (3)$$

#### B. Leg Inverse Kinematics

Assuming  $q_3 > 0$ ,  $-\sqrt{y^2 + z^2 - l_1^2} < 0$ , the inverse kinematics of the legs is given by:

$$\alpha = \cos^{-1} \frac{|z|}{\sqrt{y^2 + z^2}}, \quad \beta = \cos^{-1} \frac{l_1}{\sqrt{y^2 + z^2}} \quad (4)$$

$$q_1 = \begin{cases} \alpha - \beta, & z > 0 \\ \pi - \alpha - \beta, & z < 0 \end{cases} \quad (5)$$

$$x' = x, \quad y' = -\sqrt{y^2 + z^2 - l_1^2}, \quad D = x'^2 + y'^2 \quad (6)$$

$$\phi = \cos^{-1} \frac{|x'|}{\sqrt{D}}, \quad \psi = \cos^{-1} \frac{l_2^2 + D - l_3^2}{2l_2\sqrt{D}} \quad (7)$$

$$q_2 = \begin{cases} \frac{\pi}{2} - \psi - \phi, & x' > 0 \\ -\frac{\pi}{2} - \psi - \phi, & x' < 0 \end{cases} \quad (8)$$

$$q_3 = \cos^{-1} \frac{l_2^2 + l_3^2 - D}{2l_2l_3} \quad (9)$$

#### C. Inverse Kinematics Scheme

The inverse kinematics scheme is defined by three tasks. The first one is to keep the base at constant height and follow a reference horizontal velocity. The second is to keep the base orientation horizontal (no pitch or roll) and follow a reference yaw angular velocity. The third task is to follow the reference trajectory of the swing feet while maintaining the feet in stance phases fixed [2][6].

The functions for all three tasks are given by:

$$\dot{\mathbf{x}}_{\text{pos}} = \mathbf{R}_b^0 \dot{\mathbf{q}}_{\text{pos}} \quad (10)$$

$$\dot{\mathbf{x}}_{\text{ang}} = \mathbf{R}_b^0 \dot{\mathbf{q}}_{\text{ang}} \quad (11)$$

$$\dot{\mathbf{x}}_1 = \mathbf{R}_b^0 \dot{\mathbf{q}}_{\text{pos}} + \mathbf{T}_1^b \times \mathbf{R}_b^0 \dot{\mathbf{q}}_{\text{ang}} + \mathbf{J}_1 \dot{\mathbf{q}}_1 \quad (12)$$

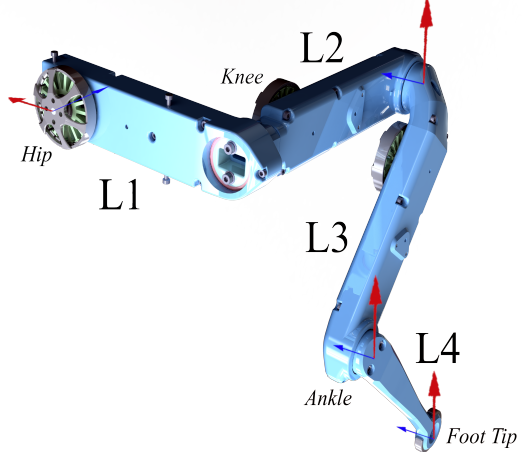


Fig. 2. Leg Parameters

$$\dot{\mathbf{x}}_2 = \mathbf{R}_b^0 \dot{\mathbf{q}}_{\text{pos}} + \mathbf{T}_2^b \times \mathbf{R}_b^0 \dot{\mathbf{q}}_{\text{ang}} + \mathbf{J}_2 \dot{\mathbf{q}}_2 \quad (13)$$

$$\dot{\mathbf{x}}_3 = \mathbf{R}_b^0 \dot{\mathbf{q}}_{\text{pos}} + \mathbf{T}_3^b \times \mathbf{R}_b^0 \dot{\mathbf{q}}_{\text{ang}} + \mathbf{J}_3 \dot{\mathbf{q}}_3 \quad (14)$$

$$\dot{\mathbf{x}}_4 = \mathbf{R}_b^0 \dot{\mathbf{q}}_{\text{pos}} + \mathbf{T}_4^b \times \mathbf{R}_b^0 \dot{\mathbf{q}}_{\text{ang}} + \mathbf{J}_4 \dot{\mathbf{q}}_4 \quad (15)$$

where  $\dot{\mathbf{q}}_{\text{pos}}$  and  $\dot{\mathbf{q}}_{\text{ang}}$  are the base linear and angular velocities in the world frame,  $\dot{\mathbf{x}}_i$  the velocity of the tip of the  $i$ th foot in world frame,  $\dot{\mathbf{q}}_{\text{pos}}$  and  $\dot{\mathbf{q}}_{\text{ang}}$  the base linear and angular velocities in the base frame,  $\dot{\mathbf{q}}_i$  the joint velocities of the  $i$ th leg,  $\mathbf{R}_b^0$  the rotation matrix from base to world frame,  $\mathbf{T}_i^b$  the position of the  $i$ th foot in the base frame, and  $\mathbf{J}_i$  the Jacobian of the  $i$ th foot.

The reference joint velocity configurations can be computed by rearranging the above equations for joint configuration velocity. The reference joint position is computed through a numerical method. The equations for the above computations are given by:

$$\mathbf{q}_i^{\text{cmd}} = \mathbf{q}_i + \mathbf{J}_i^{-1} [(\mathbf{x}_i^{\text{des}} - \mathbf{x}_i) - (\mathbf{x}_{\text{pos}}^{\text{des}} - \mathbf{x}_{\text{pos}}) - (\mathbf{T}_i^b \times \mathbf{R}_b^0) \mathbf{R}_b^0 (\mathbf{x}_{\text{ang}}^{\text{des}} - \mathbf{x}_{\text{ang}})] \quad (16)$$

$$\dot{\mathbf{q}}_i^{\text{cmd}} = \mathbf{J}_i^{-1} [\dot{\mathbf{x}}_i^{\text{des}} - \dot{\mathbf{x}}_{\text{pos}}^{\text{des}} - (\mathbf{T}_i^b \times \mathbf{R}_b^0) \mathbf{R}_b^0 \dot{\mathbf{x}}_{\text{ang}}^{\text{des}}] \quad (17)$$

where  $\mathbf{q}_i^{\text{cmd}}$  and  $\dot{\mathbf{q}}_i^{\text{cmd}}$  are the reference (command) joint positions and velocities for the  $i$ th leg,  $\mathbf{q}_i$  the current joint positions for the  $i$ th leg obtained from the state estimator,  $\mathbf{x}_i^{\text{des}}$  and  $\mathbf{x}_i$  the desired and current joint positions for the  $i$ th leg in the world frame,  $\mathbf{x}_{\text{pos}}^{\text{des}}$  and  $\mathbf{x}_{\text{pos}}$  the desired and current base linear positions in the world frame,  $\mathbf{x}_{\text{ang}}^{\text{des}}$  and  $\mathbf{x}_{\text{ang}}$  the desired and current base angular positions in the world frame,  $\dot{\mathbf{x}}_i^{\text{des}}$  the desired joint velocities for the  $i$ th leg in the world frame,  $\dot{\mathbf{x}}_{\text{pos}}^{\text{des}}$  and  $\dot{\mathbf{x}}_{\text{ang}}^{\text{des}}$  the desired base linear and angular velocities in the world frame.

Note that the desired base linear and angular velocities are determined by the user (or by a global planner) and the desired foot positions and velocities are determined by the swing trajectory generator, which we expand on in the *Foot Step Planner* section. The position of the  $i_{\text{th}}$  foot in the base frame,  $\mathbf{T}_i^b$ , is given by the forward kinematics of the feet, which is expanded on in the *Leg Forward Kinematics* subsection. The rotation matrix from base to world frame,  $\mathbf{R}_b^0$ , as well as the current base and joints positions and velocities, are estimated using the State Estimator.

#### D. Inverse Dynamics

### IV. MODEL PREDICTIVE CONTROL

The objective of our MPC is to find reaction forces which would allow our robot to follow a given trajectory. By applying several simplifications to the inverse dynamics (i.e., approximating the multi-body system as a rigid body with instantaneous states to keep the system time-varying linear), the approach keeps the formulation convex, and hence, the problem is fast to solve and furthermore, can be solved by a unique global minimum.

#### A. Gait Generator

Our architecture makes use of a symmetric forward wave gait generator which outputs the phase offsets  $\Psi$  of each leg  $i$  for a given gait template, duty factor  $\beta$  and crab angle  $\alpha$ . The generator works by linearly interpolating predefined phase offsets at known duty factors to find a computationally inexpensive approximation of the true continuous kinematic phase function.

$$\Psi_i(\alpha, \beta) = \left[ 4 \left( \left( \beta - \frac{1}{2} \right) \Psi \left( \alpha, \frac{3}{4} \right) - \left( \beta - \frac{3}{4} \right) \Psi \left( \alpha, \frac{1}{2} \right) \right) \right]_{\text{mod}i} \quad (18)$$

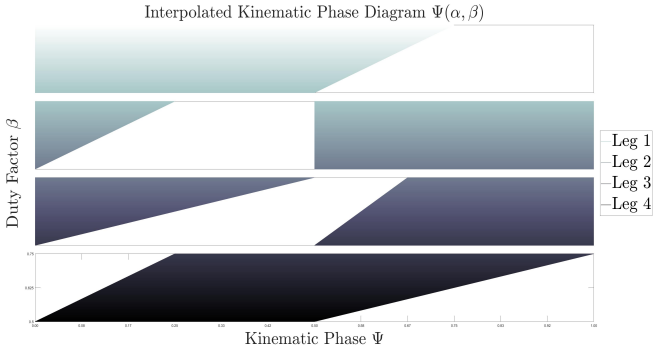


Fig. 3. **Interpolated Phase Offsets:** A trot gait with  $\alpha = 0^\circ$  for  $0.5 \leq \beta \leq 0.75$

The resulting gait function is smooth [13], and thus, we do not have to deal with the jerky gait transitions that hard coded gaits suffer from. With the ability to alter the actual duty factor and crab angle of the legs in real time, our approach offers the possibility of both higher stability and higher stable

velocities because the gait generator can optimize the duty factor to reach a desired stability margin, without relying on changing the constraints of the leg trajectory generators.

#### B. Foot Step Planner

The goal of the footstep planner is to identify the trajectory of each foot while in swing phase. The target location at each cycle is given by:

$$\mathbf{r}_i^{\text{cmd}} = \mathbf{p}_{\text{shoulder},i} + \mathbf{p}_{\text{symmetry}} + \mathbf{p}_{\text{centrifugal}} \quad (19)$$

where,

$$\mathbf{p}_{\text{shoulder},i} = \mathbf{p}_k + \mathbf{R}_z(\psi_k) \mathbf{l}_i, \quad (20)$$

$$\mathbf{p}_{\text{symmetry}} = \frac{t_{\text{stance}}}{2} \mathbf{v} + k (\mathbf{v} - \mathbf{v}^{\text{cmd}}), \quad (21)$$

$$\mathbf{p}_{\text{centrifugal}} = \frac{1}{2} \sqrt{\frac{h}{g}} \mathbf{v} \times \boldsymbol{\omega}^{\text{cmd}} \quad (22)$$

Note that in the simplest case (without centripetal velocities, and while the robot is perfectly tracking the reference velocity),  $\mathbf{r}_i^{\text{cmd}}$  is simply the summation of the position of the body w.r.t world, the projection of the position of the local hip frame onto the XZ world plane w.r.t the body, and half of the body displacement w.r.t world between the  $k$  and  $k+1$  time-step.

To satisfy this trajectory at the potentially variable frequency of the gait scheduler, we have imposed three constrained polynomial trajectories on each leg (one for each component in  $\mathbb{R}^3$ ), with the two horizontal polynomial trajectories being 5<sup>th</sup> order to control the position, velocity, and acceleration initial and final setpoints. The vertical trajectory is a 6<sup>th</sup> order polynomial and has an additional positional constraint which allows for parameterization of the zenith.

### V. IMPLEMENTATION DETAILS

### VI. RESULTS

#### A. Experimental Setup

This project's simulation platform consists of the open-source Robot Operating System (ROS), Gazebo, and Rviz. During the initial stage of our project, we utilized ROS and Gazebo to spawn our robot and control the position of its legs in the physics simulator.

#### B. Simulation

A universal robot description format (URDF) of the robot was created using the STL model of the robot. The URDF was spawned in Gazebo using a launch file, and utilized a controller manager for primitive joint control. The URDF spawned in Gazebo is shown below:

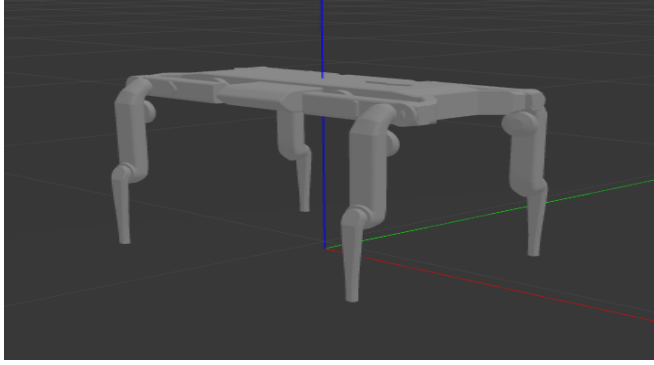


Fig. 4. **Solo-12 in Gazebo:** Spawned URDF

## VII. CONCLUSIONS AND FUTURE WORK

### REFERENCES

- [1] Kim, Donghyun & Carlo, Jared & Katz, Benjamin & Bledt, Gerardo & Kim, Sangbae. (2019). Highly Dynamic Quadruped Locomotion via Whole-Body Impulse Control and Model Predictive Control.
- [2] P. -A. Léziart, T. Flayols, F. Grimminger, N. Mansard and P. Souères, "Implementation of a Reactive Walking Controller for the New Open-Hardware Quadruped Solo-12," 2021 IEEE International Conference on Robotics and Automation (ICRA), 2021, pp. 5007-5013, doi: 10.1109/ICRA48506.2021.9561559.
- [3] [https://github.com/open-dynamic-robot-initiative/open\\_robot\\_actuator\\_hardware](https://github.com/open-dynamic-robot-initiative/open_robot_actuator_hardware)
- [4] Yan, Wei et al. "Whole-body kinematic and dynamic modeling for quadruped robot under different gaits and mechanism topologies." PeerJ Computer Science 7 (2021): n. pag.
- [5] J. Di Carlo, P. M. Wensing, B. Katz, G. Bledt, and S. Kim, "Dynamic Locomotion in the MIT Cheetah 3 Through Convex Model-Predictive Control," in IEEE/RSJ International Conference on Intelligent Robots and Systems (IROS). IEEE, 2018, pp. 1-9.
- [6] H.-W. Park, P. M. Wensing, and S. Kim, "High-speed bounding with the MIT Cheetah 2: Control design and experiments;" The International Journal of Robotics Research, vol. 36, no. 2, pp. 167-192, Mar. 2017.
- [7] D. Kim, J. Lee, J. Ahn, O. Campbell, H. Hwang, and L. Sentis, "Computationally-Robust and Efficient Prioritized Whole-Body Controller with Contact Constraints," in IEEE/RSJ International Conference on Intelligent Robots and Systems (IROS), 2018.
- [8] G. Bledt, P. M. Wensing, S. Ingersoll, and S. Kim, "Contact model fusion for event-based locomotion in unstructured terrains," in IEEE International Conference on Robotics and Automation (ICRA), May 2018, pp. 1-8.
- [9] D. Kim, S. Jorgensen, J. Lee, J. Ahn, J. Luo, and L. Sentis, "Dynamic Locomotion For Passive-Ankle Biped Robots And Humanoids Using Whole-Body Locomotion Control," arXiv.org, Jan. 2019.
- [10] S. Caron, Q.-C. Pham, and Y. Nakamura, "Stability of Surface Contacts for Humanoid Robots: Closed-Form Formulae of the Contact Wrench Cone for Rectangular Support Areas," arXiv.org, Jan. 2015.
- [11] J. Carpentier, M. Benallegue, N. Mansard, and J.-P. Laumond, "A kinematics-dynamics based estimator of the center of mass position for anthropomorphic system—a complementary filtering approach," in IEEE-RAS 15th International Conference on Humanoid Robots(Humanoids), 2015, pp. 1121-1126.
- [12] J. Di Carlo, P. M. Wensing, B. Katz, G. Bledt and S. Kim, "Dynamic Locomotion in the MIT Cheetah 3 Through Convex Model-Predictive Control," 2018 IEEE/RSJ International Conference on Intelligent Robots and Systems (IROS), 2018, pp. 1-9, doi: 10.1109/IROS.2018.8594448.
- [13] K. Yoneda, K. Suzuki and Y. Kanayama, "Gait planning for versatile motion of a six legged robot," Proceedings of the 1994 IEEE International Conference on Robotics and Automation, 1994, pp. 1338-1343 vol.2, doi: 10.1109/ROBOT.1994.351302.